Original Research

Slow-cycling murine melanoma cells display plasticity and enhanced tumorigenicity in syngeneic transplantation assay

Anna Kusienicka [a,*], Maciej Cieśla [a], Karolina Bukowska-Strakova [a,b], Witold Norbert Nowak [a], Iwona Bronisz-Budzyńska [a], Agnieszka Seretny [a], Monika Żukowska [a], Mateusz Jeż [a], Jan Wolnik [a], Alicja Józkowicz [a]

[a] Department of Medical Biotechnology, Faculty of Biophysics, Biochemistry and Biotechnology, Jagiellonian University, 30-387 Krakow, Poland
[b] Department of Clinical Immunology, Institute of Pediatrics, Jagiellonian University Medical College, 31-663 Krakow, Poland

A R T I C L E   I N F O

A B S T R A C T

Slow-cycling cancer cells (SCC) contribute to the aggressiveness of many cancers, and their invasiveness and chemoresistance pose a great therapeutic challenge. However, in melanoma, their tumor-initiating abilities are not fully understood. In this study, we used the syngeneic transplantation assay to investigate the tumor-initiating properties of melanoma SCC in the physiologically relevant *in vivo* settings. For this we used B16-F10 murine melanoma cell line where we identified a small fraction of SCC. We found that, unlike human melanoma, the murine melanoma SCC were not marked by the high expression of the epigenetic enzyme *Jarid1b*. At the same time, their slow-cycling phenotype was a temporary state, similar to what was described in human melanoma. Progeny of SCC had slightly increased doxorubicin resistance and altered expression of melanogenesis genes, independent of the expression of cancer stem cell markers. Single-cell expansion of SCC revealed delayed growth and reduced clone formation when compared to non-SCC, which was further confirmed by an *in vitro* limiting dilution assay. Finally, syngeneic transplantation of 10 cells *in vivo* established that SCC were able to initiate growth in primary recipients and continue growth in the serial transplantation assay, suggesting their self-renewal nature. Together, our study highlights the high plasticity and tumorigenicity of murine melanoma SCC and suggests their role in melanoma aggressiveness.

Introduction

Melanoma is the most aggressive skin cancer worldwide, responsible for around 57 000 deaths annually [1]. When diagnosed early, it is almost 100% curable, but late stage disease poses a big therapeutic challenge due to the unique heterogeneity and plasticity of melanoma cells [2]. One of the factors contributing to melanoma therapy resistance is the presence of slow-cycling cancer cells (SCC) [3]. Unlike terminally differentiated cells that are irreversibly arrested in G0/G1 phase (e.g. muscle cells or neurons), SCC are only transiently arrested in G0/G1 phase and can re-enter the cell cycle upon stimulus [4]. Importantly, those quiescent SCC are difficult to eradicate and might be responsible for cancer relapse as chemo- and radiotherapies target highly proliferative cancer cells [4].

Human melanoma SCC are highly invasive and disseminate from the primary tumor mass in the early stages of the disease [5]. They express epigenetic enzymes JARID1B and TET2, have an active WNT5A signaling, and support continuous tumor growth and chemoresistance [6–9]. Interestingly, the slow-cycling phenotype partially overlaps with the properties of cancer stem cells (CSC) which are believed to be plastic tumor-initiating cells that self-renew and give rise to highly proliferating cells of the tumor mass [4]. However, in melanoma, the existence of CSC (called melanoma initiating cells, MIC) is controversial. It was shown that MIC are not rare and that MIC markers do not enrich for enhanced tumorigenic potential [10,11].

Most of the studies test initiating properties of melanoma cells using immunocompromised mice. Interestingly, the degree of immunodeficiency of mice significantly affects the outcome of the assay. The more immunodeficient the mouse strain is, the more susceptible it is to melanoma formation. Thus there is a need for validation of the tumorigenic potential of melanoma cells in models with intact immune systems and humanized mice models [10,12]. Recently, we have addressed

this issue and checked the tumorigenicity of cells expressing MIC markers (CD20, ALDH[high]) in murine melanoma using syngeneic transplantation assay in immunocompetent C57BL/6 mice. Our results showed that melanoma cells are highly tumorigenic regardless of the expression of MIC markers, confirming observations from human melanoma [13]. However, the tumorigenic status of SCC in the presence of an intact immune system still remains unknown.

In this study, we addressed this gap in knowledge and tested the tumor initiating properties of SCC in the presence of an intact immune system. For this purpose we identified and characterized SCC in murine melanoma B16-F10 cell line and studied their tumorigenicity in syngeneic serial transplantation assay. Using the PKH26 dye retention technique we distinguished a small subpopulation of PKH26-retaining cells. We found that they are temporary plastic cells that give rise to dividing progeny with slightly enhanced chemoresistance and altered expression of melanogenesis genes *in vitro*. We observed that despite lower *in vitro* clonogenicity of SCC, they show higher *in vivo* tumorigenicity compared to control cells. Our results provide insight into the high plasticity of SCC in murine melanoma and indicate their role in melanoma maintenance and aggressiveness.

Materials and methods

Cell culture

B16-F10 murine melanoma cells (ATCC) were cultured in standard conditions (5% CO_2, 37°C, 95% humidity) in RPMI 1640 medium (Lonza) supplemented with 10% fetal bovine serum (FBS; Eurx), 1% of Penicillin-Streptomycin (stock 10,000 units/mL of penicillin and 10 mg/mL streptomycin, Sigma-Aldrich) and 2 mM L-glutamine (Lonza). The passage was performed every 2-3 days when cells reached around 90% confluency.

Animals

The C57BL/6-Tg(UBC-GFP)30Scha/J mice used in this study were purchased from The Jackson Laboratory and bred in the Specific Pathogen Free (SPF) Animal Facility of the Faculty of Biochemistry, Biophysics and Biotechnology at the Jagiellonian University. Mice were housed in individually ventilated cages and monitored in accordance with the recommendations of the Federation of European Laboratory Animal Science Association (FELASA). All procedures were approved by the II Local Ethical Committee for Animal Experiments in Krakow (approval number 139/2015).

Generation of stable B16-F10 cell line expressing firefly luciferase (Luc) transgene

Generation of B16-F10 Luc cell line was performed as previously described [13]. Briefly, HEK293 cells were transfected with PGK V5-Luc Neo, psPAX2 and pMD2.G plasmids (Addgene) using polyethyleneimine (Polysciences Inc.) to generate lentiviral vectors (LVs). After 48 h, medium with LVs was used for transduction of B16-F10 cells, and transduced cells were selected with 0.8 mg/ml G418 (CytoGen GmbH). To obtain a stable clonal cell line with high luciferase activity, single transduced cells were sorted into 96-well plates for clonogenic growth using MoFlo XDP (Becton Dickinson) cell sorter. Obtained clones were checked for luciferase activity using In Vivo Imaging System (IVIS) Lumina (PerkinElmer) and highly positive clones were pooled and regarded as a stable cell line for further experiments.

PKH26 staining

B16-F10 cells were stained with PKH26 dye (Sigma-Aldrich). Two million cells were suspended in 0.5 ml diluent C (provided by the manufacturer). In another tube, 2 μl of PKH26 dye was added to 0.5 ml diluent C. Both solutions were immediately mixed and cells were incubated

for 5 minutes at room temperature (RT). The staining was stopped using 10 ml RPMI complete medium, centrifuged (300g, 5 min) and washed twice with PBS without ions before further culture.

ALDH activity and CD133 staining

One million cells were stained for 30 minutes at 37°C with ALDEFLUOR[TM] kit (STEMCELL Technologies) according to the vendor's protocol. Cells were subsequently stained with DAPI (0.2 μg/ml, Sigma-Aldrich; 20 min, 4°C). Separate staining for CD133 was performed using anti-mouse CD133 APC antibody (clone 315-2C11, BioLegend) and 0.2 μg/ml DAPI (Sigma-Aldrich) (20 min, 4°C). Cells were analyzed using BD LSRFortessa (BD Bioscience) flow cytometer.

Cell cycle analysis

To identify cells in the G0 phase within the PKH26^{+} and PKH26^{−} subpopulations, we used BD IntraSureTM Kit (BD Biosciences) according to the vendor's protocol. In short, after fixation and lysis, cells were stained (15 min, RT in the dark) with 1 μl of anti-Ki67 antibody (clone 16A8, BioLegend, 1:100 dilution). After washing with PBS, cells were stained (10 min, RT in the dark) with 100 μg/ml Hoechst 33342 (Sigma-Aldrich). Samples were immediately analyzed using BD LSRFortessa (BD Bioscience) flow cytometer.

Gene expression analysis from a limited number of cells using AmpliGrid System

PKH26[+] and PKH26^{−} cells were sorted using MoFlo XDP (Becton Dickinson) cell sorter on AmpliGrid (Beckman Coulter) Single Cell PCR Slide (50 cells/reaction site, 4-6 sites per condition) as described previously [13]. Slides were dried overnight at 4°C and reverse transcription was performed using NCode Vilo kit (Invitrogen, 1 μl mix/reaction site + 5 μl of sealing oil) in the AmpliSpeed ASC200D slide cycler (Advalytix). Diluted cDNA (10x) was used for quantitative Real-Time PCR (qRT-PCR) analysis with SYBR® Green JumpStart[TM] Taq ReadyMix[TM] (Sigma-Aldrich) in the StepOne Plus PCR (Applied Biosystems) cycler according to the vendor's protocol. *Ef2* was used as a reference gene. Sequences of primers are listed in Supplementary Table 1.

RT² Profiler[TM] PCR Array

For RT² Profiler[TM] PCR Array 10 000 PKH26^{+} and 10 000 PKH26^{−} cells (selected 12 days after PKH26 staining) were sorted into 100 μl Buffer RL (Norgen) as described before [13]. RNA was isolated with Single Cell RNA Purification Kit (Norgen) with On-Column DNA Removal (Norgen) followed by reverse transcription PCR using NCode Vilo (Invitrogen). RT² Profiler[TM] PCR Array (Qiagen) detecting murine CSC-related genes was performed using the vendor's protocol and StepOne Plus PCR (Applied Biosystems) cycler. Genes included in the array are listed in Supplementary Table 2.

In vitro clonogenic test and obtaining clonogenic cell lines

Single PKH26^{+} and PKH26^{−} cells (selected 12 days after PKH26 staining) were sorted into 96-well plates with MoFlo XDP (Becton Dickinson) cell sorter. Cells were cultured in melanoma initiating cells medium (MIC) [14] and pictures were taken every second day (from day 5). Established clones were counted after two weeks of culture and further cultivated in the MIC medium for progeny analyses.

In vitro extreme limiting dilution assay (ELDA)

For the primary ELDA, PKH26^{+} and PKH26^{−} cells (selected for 12 days after PKH26 staining) were sorted using MoFlo XDP (Becton Dickinson) cell sorter into 96-well plate (1, 3, 5, 7, or 10 cells/well,

12 wells for each condition) and cultured in the MIC medium. Positive wells were counted after two weeks of culture. For the secondary ELDA, single PKH26$^+$ and PKH26$^-$ cells were sorted and cultured in the MIC medium. After clone formation, single clones (3 PKH26$^+$ and 3 PKH26$^-$) were sorted for ELDA in the same scheme as the primary ELDA. Data analysis was performed using http://bioinf.wehi.edu.au/software/elda/index.html.

Quantitative RT Polymerase Chain Reaction (qRT-PCR)

Gene analysis of progeny of PKH26$^+$ and PKH26$^-$ cells was performed on RNA isolated with phenol–chloroform extraction as described previously [15]. The RNA concentration was measured using a Nanodrop ND-1000 spectrophotometer, and reverse transcription was performed using the RevertAid First Strand cDNA Synthesis Kit (Thermo Scientific) followed by qRT-PCR using the SYBR Green JumpStart Taq ReadyMix (Sigma-Aldrich) and StepOnePlus thermocycler according to the vendors' protocols. Sequences of primers are listed in Supplementary Table 1.

MTT assay

Cell lines obtained from PKH26$^+$ and PKH26$^-$ clones were seeded in 96-well plates (1500 cells/well, in triplicates) in culture medium. After 24 hours, medium was exchanged for RPMI supplemented with 0.1, 0.5 or 1 μM doxorubicin (Sigma-Aldrich). After 24 h treatment, medium was exchanged for RPMI supplemented with 1 mg/ml thiazolyl blue tetrazolium bromide (MTT, Sigma-Aldrich), cells were incubated 20 minutes in 37°C and after removal of medium, cells were lysed with lysis buffer (10 g SDS and 0.6 ml 100% acetic acid in 100 ml DMSO) and absorbance was read at 562 nm using Tecan Infinite M200 Pro Reader (Mannedorf).

In vivo *serial transplantation of cells*

Primary *in vivo* transplantation of PKH26$^+$ and PKH26$^-$ cells was performed 12 days after PKH26 staining. Cells were stained with 0.2 μg/ml DAPI and live PKH26$^+$ or PKH26$^-$ cells were sorted into tubes to obtain 10 cells per 100 μl in 1:1 PBS in Matrigel GFR (Corning) solution. C57BL/6-Tg(UBC-GFP)30Scha/J male mice (n=10-11) were injected subcutaneously (2 plugs/mouse) with 100 μl of cell suspension under isoflurane anesthesia (Baxter). Mice were euthanized when tumors reached 1 cm in diameter and tumors were excised, digested, and stained with Hoechst 33342 (Sigma-Aldrich) and 7-AAD (BD Pharminogen) as previously described [13,16]. GFP$^-$7AAD$^-$Hoechst$^+$ tumor cells were sorted (into 1:1 PBS in Matrigel GFR solution) to obtain 100 cells per 100 μl. Each primary tumor was injected into 9–10 C57BL/6-Tg(UBC-GFP)30Scha/J secondary recipients (100 μl of cell suspension, 2 plugs/mouse). The same was done for tertiary transplantations, but each secondary tumor was transplanted to one tertiary recipient.

In vivo *detection of bioluminescence*

The tumor growth was monitored using IVIS Lumina (PerkinElmer) once a week starting on day 16. Briefly, 20 minutes before imaging mice were injected intraperitoneally (i.p.) with 150 μl of luciferin (15 mg/ml, TriMen Chemicals). Five minutes before measurement mice were anesthetized with isoflurane (Baxter) and 2 minute exposure time was used for detection of bioluminescence.

Post-mortem *detection of metastases*

When tumors reached around 1 cm in diameter, mice were injected i.p. with 150 μl of the luciferin (15 mg/ml, TriMen Chemicals) and euthanized 20 minutes later. Liver, intestine, lungs and spleen were excised, put on the culture dish, and luminescence signal was measured with IVIS Lumina (PerkinElmer).

Measurement of ALDH activity in tumor samples

50,000-250,000 GFP$^-$7AAD$^-$Hoechst$^+$ tumor cells were sorted and used for ALDEFLUOR^{TM} (STEMCELL Technologies) staining according to the vendor's protocol (but scaled down to 1 μl of reagents and 200 μl of assay buffer). Cells were additionally stained with 7-AAD (BD Pharminogen; 10 min, RT in the dark) for the detection of dead cells and analyzed using BD LSRFortessa (BD Bioscience) flow cytometer.

Statistical analysis

Prism 9 for Mac OS (GraphPad Software) and Microsoft Excel for Mac (Microsoft Office 365, Excel version 16) software were used for data analysis. For comparison of two groups two-tailed Student t-test was used, for three groups one-way or two-way ANOVA with Bonferroni post-test, and for clonogenic analysis two-tailed Fisher exact test. Mann–Whitney test was used for comparison of two groups with non-normal distribution.

Results

Identification of PKH26 label-retaining cells in B16-F10 murine melanoma cell line

To study the biology of murine SCC we used PKH26 membrane labeling dye that stains all cells uniformly and is diluted with every cell division [5,6,17–19]. Flow cytometry analysis showed a rapid dilution of PKH26 dye in most of B16-F10 cells. On day 6 after staining, we observed two fractions of PKH26$^+$ cells (low and high), and on day 10 only around 0.1% of cells remained PKH26$^+$ (Fig. 1A). The microscopic observations showed no morphological differences between PKH26$^-$ and PKH26$^+$ cells (Fig. 1B).

Slow-cycling phenotype can be one of the hallmarks of CSC [20]. Using flow cytometry analysis of MIC markers expression, we found increased percentages of CD133$^+$ and ALDH^{high} cells within PKH26$^+$ subpopulation (Fig. 1C). Interestingly, cell cycle analysis 7 days after PKH26 staining showed that PKH26^{high} cells are not enriched in the G0 phase cells when compared to the PKH26^{dim} fraction (Fig. 1D). This suggests that murine melanoma SCC represent a transient cell population, which proliferate but to a lesser extent than non-SCC.

We next determined levels of mRNAs previously linked to CSC phenotype (Supplementary Table 2). Of the 53 expressed CSC-associated genes, no gene was significantly changed in murine SCC, including epigenetic modifiers *Id1, Dnmt1* and *Hdac1* known to be associated with slow-cycling state (Fig. 1E) [21–23]. In addition, we analyzed the expression of *Jarid1b*, the marker of human melanoma SCC [6], and observed no differences between SCC and non-SCC (Fig. 1F). Further, to check whether SCC exhibit altered melanoma differentiation status we examined expression of microphthalmia-associated transcription factor (*Mitf*) – a master regulator of melanogenesis, and tyrosinase (*Tyr*) – the key melanogenesis enzyme. The analysis revealed no changes in expression of these genes in SCC, suggesting that the differentiation status of these cells is not altered in murine melanoma (Fig. 1F).

In vitro *clonogenic potential of PKH26$^+$ murine melanoma cells*

We then performed a single-cell sort of PKH26$^+$ and PKH26$^-$ cells 12 days after staining and tested the ability of SCC to grow as single cell-derived clones in serum-free MIC medium that supports the growth of stem cell-like cells [14] (Fig. 2A). On day 5, PKH26$^+$ clones had fewer cells than PKH26$^-$ clones, indicating a slower proliferation rate (Fig. 2B). Moreover, the PKH26$^+$ cells had reduced ability to form clones and generated fewer and smaller clones than the PKH26$^-$ cells (Fig. 2C and D). They were able to form more than one clone per well, indicating that at some point cells disseminated from the primary clone to form satellite clones due to differences in migration or de-adhesion of
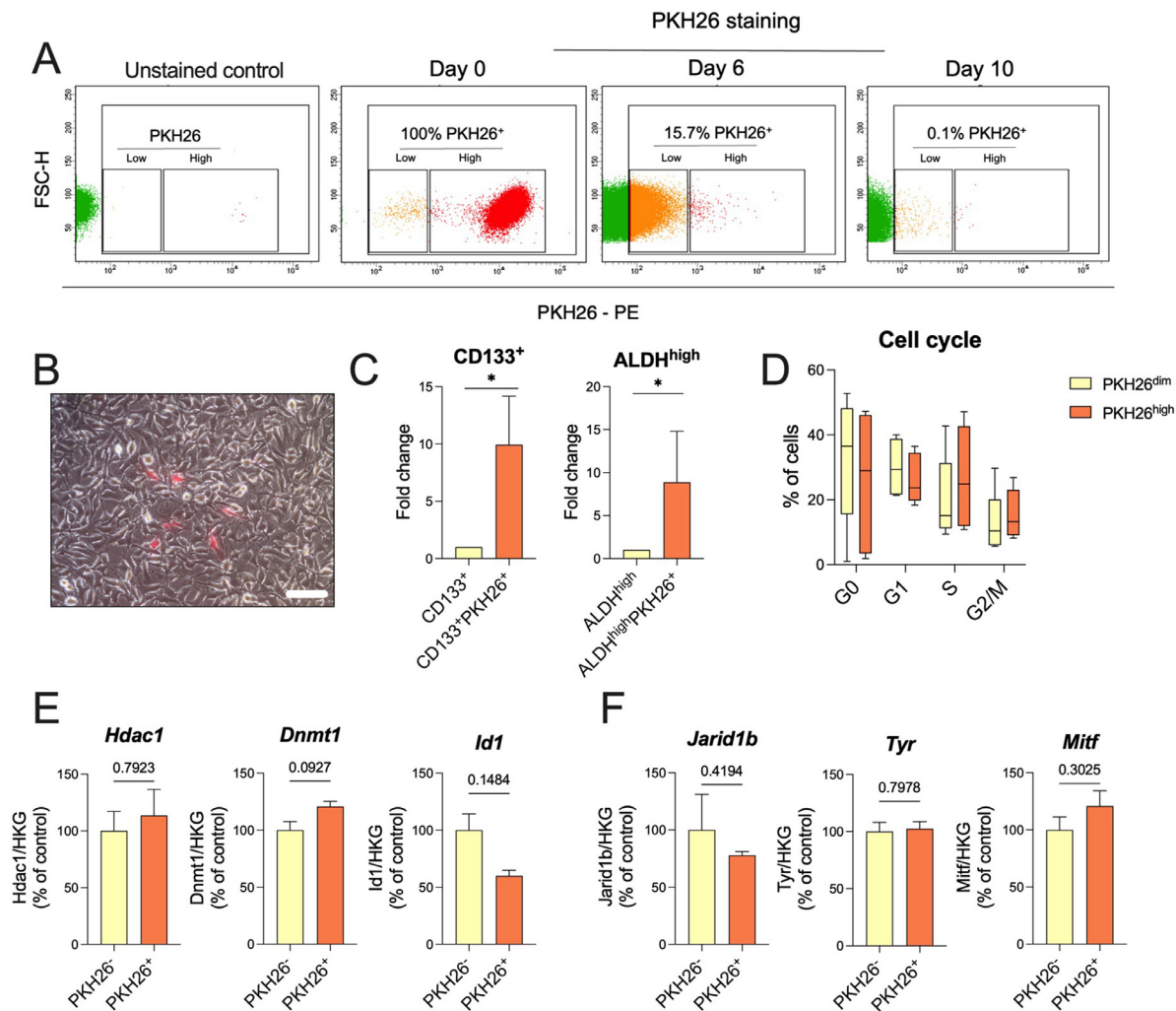
Fig. 1. Identification of PKH26+ cells in B16-F10 murine melanoma cell line; **A.** Flow cytometry analysis of PKH26 fluorescence in B16-F10 cells. Representative FACS scatter plots. **B.** Representative microscopic view of PKH26+ cells 6 days after staining (multichannel picture, scale bar = 100 μm). **C.** Flow cytometry of CD133 and ALDH activity 7 days after PKH26 staining. Data are presented as the fold change of the CD133+ or ALDH^{high} expression in PKH26+ fraction vs. CD133+ or ALDH^{high} in all cells, n=4, each bar represents mean + SEM,* - p<0.05 vs. control. **D.** Flow cytometry analysis of the cell cycle 7 days after PKH26 staining. Box and whisker plots with median value, n=5; **E.** Gene expression analysis of *Hdac1, Dnmt1* and *Id1* (RT^2 Profiler^{TM} PCR Array, Qiagen), each bar represents mean + SEM, average of 5 housekeeping genes (HKG) used as a reference, n=2. **F.** Gene expression analysis of *Jarid1b, Tyr* and *Mitf*. qRT-PCR analysis on 50 sorted cells, after pre-amplification with the AmpliGrid system, *Ef2* was used as a reference gene, each bar represents mean + SEM, n=3-6.

cells (Fig. 2E). However, detailed analysis using time lapse recording on day 8 after sort revealed no differences in track length and velocity of migrating spheres and clone cells (Supplementary Fig. 1). This suggests that satellite clone formation might be independent of migratory potential or occurs in the early stages of clonogenic growth that we did not detect in our experimental settings.

Our clonogenic assay revealed that murine B16-F10 melanoma cells have a high ability to grow as clones from single cells, confirming what we observed previously [13] and what has been observed in human melanoma [10]. To estimate the exact active fraction of clone initiating cells, we performed an extreme limiting dilution assay (ELDA) *in vitro*. PKH26− and PKH26+ cells were sorted in different numbers and grown in MIC medium. Positive wells were counted after two weeks of culture and frequency of clone initiating cells was calculated using ELDA software [24]. The results show that SCC have almost two times smaller fraction of clone initiating cells than control cells (1/8.44 vs. 1/4.43, Fig. 2F) which is in agreement with results of clonogenic assay. To verify if the frequency of clone initiating cells remained unaffected, single PKH26− and PKH26+ cells from primary clone formation were sorted for secondary ELDA assay. Despite the detection of fewer positive wells,

the trend for decreased clonogenic potential of PKH26+ cells was unchanged in the secondary ELDA (Fig. 2F).

Characterization of the progeny of PKH26− and PKH26+ clones

We then characterized the cell lines derived from PKH26− and PKH26+ clones. First, we checked whether progeny of PKH26+ cells was enriched for SCC. To verify this, we performed PKH26 staining of PKH26− and PKH26+-derived cell lines and analyzed the percentage of SCC after 10 days of culture. We detected PKH26+ cells in all cell lines without significant differences in the percentage of PKH26+ cells between two groups (Fig. 3A). Interestingly, progeny of PKH26− consisted of both PKH26− and PKH26+ cells. This once again suggests that the slow-cycling phenotype in murine melanoma is rather a transient state that cells may acquire, consistent with the results from human melanoma [6]. Additionally, we checked whether SCC-derived cell lines were enriched with MIC cells. Flow cytometry analysis of ALDH activity showed no differences between PKH26− and PKH26+-derived cell lines in ALDH^{high} fraction (Fig. 3B).
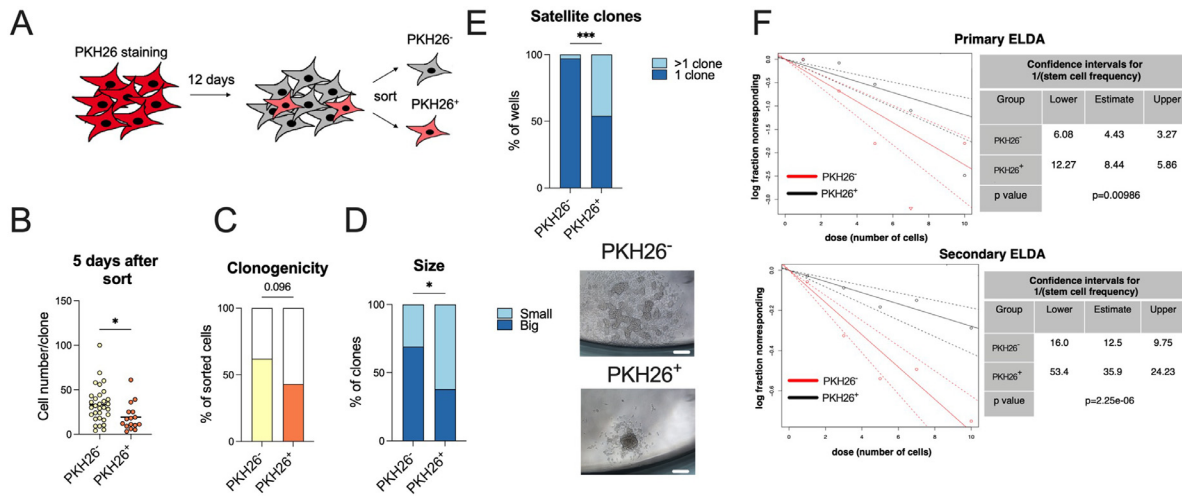
Fig. 2. Evaluation of *in vitro* clonogenic potential of PKH26+ and PKH26− cells; **A.** Scheme of sorting of PKH26+ and PKH26− cells for clonogenic assays. **B.** Number of cells per clone, 5 days after sorting. Data represented as individual values and mean, n=16-31, * - p<0.05. **C.** Number of clones formed by PKH26− and PKH26+ single cells 13 days after sorting. **D.** Size of PKH26+ and PKH26− clones 13 days after sorting and representative pictures of clones at day 11 (scale bar = 100 μm). **E.** Satellite clones formation 13 days after sort calculated as a % of wells in 96-well plate that had more than one clone, *** - p<0.001. **F.** Primary and secondary ELDA. Trend lines represent the estimated frequency of active cells that are able to form clones, and dotted lines represent 95% confidence intervals.
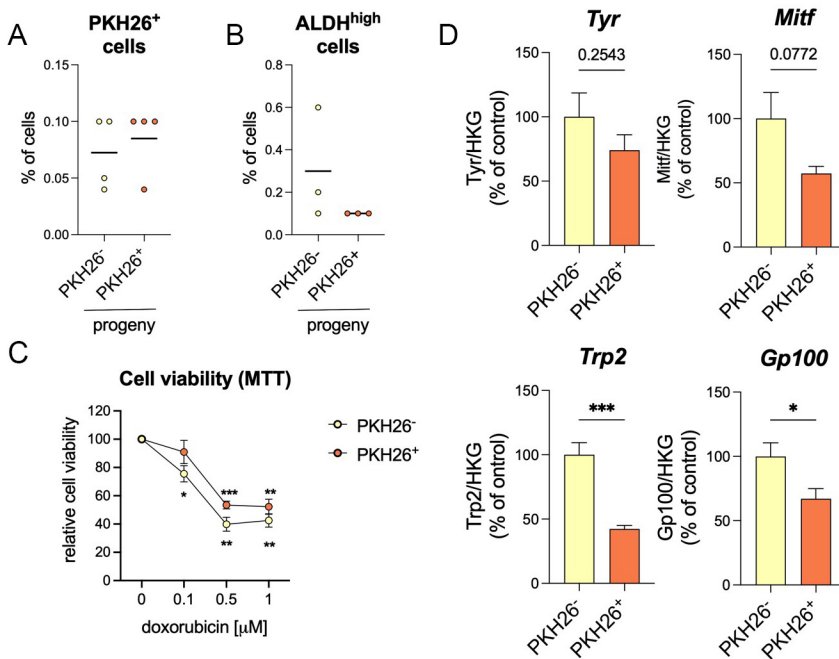

Fig. 3. Characterization of PKH26+ and PKH26− -derived cell lines; Flow cytometry analysis of (**A**) PKH26 retaining ability and (**B**) ALDH^{high} fraction in the PKH26− and PKH26+ progeny. **C.** Effect of doxorubicin (24 h treatment) on the viability of PKH26− and PKH26+ progeny. MTT reduction assay, each point represents mean ± SEM, n=4, * - p<0.05, ** - p< 0.01, *** - p< 0.001 versus untreated cells. **D.** Gene expression of MAAs. qRT-PCR analysis, *Ef2* was used as a housekeeping control; each bar represents mean + SEM; n=5-6, * - p<0.05, *** - p< 0.001.

Chemotherapeutics target proliferating cancer cells and the slow-cycling phenotype may contribute to chemoresistance in cancers, including melanoma [7,25]. To test if SCC progeny differed in response to chemotherapy, PKH26− and PKH26+-derived cell lines were treated with doxorubicin. Already at the lowest 0.1 μM concentration of doxorubicin, the PKH26− progeny had significantly reduced viability, which was not the case for the PKH26+ progeny (Fig. 3C). At higher doxorubicin concentrations, PKH26+ progeny tended to be more chemoresistant than PKH26− progeny, but this was not statistically significant (Fig. 3C).

The differentiation status of melanoma is an important prognostic factor for disease outcome [26]. We checked the expression of several melanoma-associated antigens (MAAs) and melanogenesis genes and found that progeny of SCC had lower mRNA levels of glycoprotein 100 (*Gp100*) and tyrosinase-related protein 2 (*Trp-2*) (Fig. 3D). This result

indicates that SCC can produce cells with altered differentiation status in murine melanoma.

In vivo evaluation of the tumorigenic potential of PKH26− and PKH26+ cells

To investigate the tumorigenic potential of murine melanoma SCC, we performed an *in vivo* syngeneic transplantation assay using C57BL/6 mice expressing green fluorescent protein (GFP) under human ubiquitin C promoter to distinguish GFP+ host cells from GFP− melanoma cells during serial transplantations. Additionally, to detect tumor initiation and growth dynamic, B16-F10 cells were transduced with firefly luciferase (Luc) transgene and monitored using IVIS system.

Mice were injected subcutaneously with 10 sorted PKH26− or PKH26+ cells (Fig. 4A). Primary transplantation resulted in tumors only
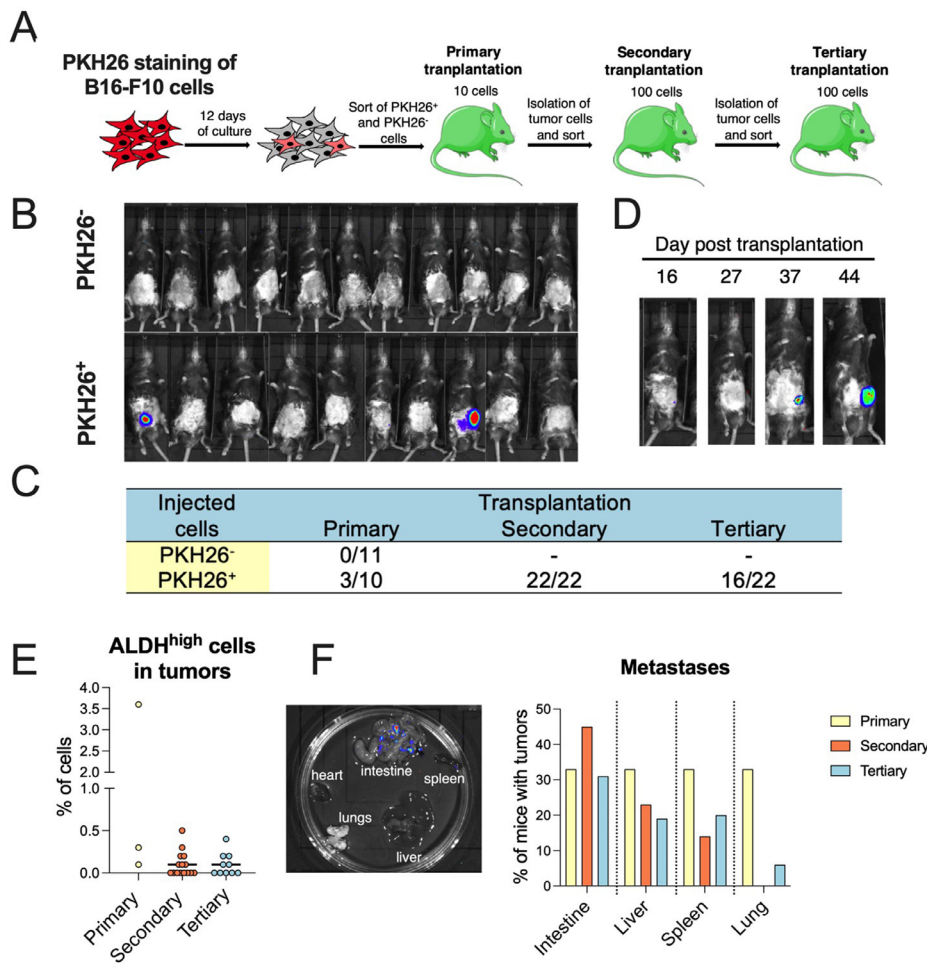
Fig. 4. *In vivo* serial transplantation of PKH26⁻ and PKH26⁺ cells. **A.** Scheme of the experiment. **B.** Luminescence of tumor cells measured with IVIS 16 days after transplantation. **C.** Table with the efficacy of tumor formation in serial transplantation assay. **D.** Luminescence measured with IVIS of the slowly proliferating tumor formed by PKH26⁺ cells in the primary recipient. **E.** Measurement of ALDH activity in tumor samples. Flow cytometry analysis, data represented as individual values and mean, n=3-15. **F.** Luminescence of tumor cells in distant organs measured *post-mortem* in mice with tumors.

in PKH26⁺ group, with 3 out of 10 injected mice with the tumor burden (Fig. 4B and C). Interestingly, one tumor developed from PKH26⁺ cells more than five weeks after transplantation, indicating quiescent phenotype of injected cells (Fig. 4D). We observed that SCC-derived tumor cells were able to form tumors in secondary and tertiary recipients, suggesting that they had the ability to self-renew and maintain tumorigenic potential (Fig. 4C). We tested the ALDH activity and observed that percentage of ALDH^high cells was heterogeneous in tumors ranging from 0% to 0.5%, with one primary recipient having 3.6% of ALDH^high cells (Fig. 4E). We did not observe any pattern of inheritance of ALDH activity as primary tumors with ALDH^high subpopulation can develop both tumors with or without ALDH^high cells (Supplementary Fig. 2). Finally, we tested the formation of metastases and detected metastatic lesions in intestines, liver, spleen and lungs in some but not all recipients (Fig. 4F). The metastatic capacity was not inherited among recipients of the same cells. Our data suggests that SCC progeny gradually lose their metastatic potential to liver and lungs during serial transplantations (Fig. 4F).

Discussion

Slow-cycling cells contribute to melanoma therapy resistance and tumor maintenance [3–6]. In this study, we characterized SCC in the murine melanoma cell line B16-F10 and transplanted SCC into syngeneic C57BL/6 mouse strain to test tumorigenic potential. Using PKH26 dye and 10-12 days of selection, we detected a small (around 0.1%) subpopulation of SCC (Fig. 1A) similarly to what was described in many types of cancers including melanoma, colorectal cancer, breast cancer and glioblastoma [5,7,18,25]. Melanoma SCC [5] as well as human colorectal cancer SCC [25] have been shown to be arrested in G2/M

phase. Additionally, like quiescent cells at G0 phase, slow-cycling cancer cells usually do not express proliferation marker Ki67 [6,7,27]. In our study we observed high variability in the cell cycle composition among PKH26⁻ and PKH26⁺ fractions and no enrichment in G0 phase in PKH26⁺ cells (Fig. 1D). This suggests that labeling with PKH26 dye identifies a temporary slow-cycling state, not a truly quiescent cell population, and that SCC proliferated more slowly but with time or stimulus they could re-enter cycling. Such a temporary state of slow divisions was previously described in human melanoma by Roesch and colleagues [6]. Moreover, melanoma cells have been shown to rapidly exit G1 phase arrest in a more favorable environment, which means that they are susceptible to rapid changes in cell cycle status [28]. Our data demonstrates a similarity in the transient nature of SCC between mouse and human melanoma, suggesting that a temporary state of this phenotype might be a general, species-independent feature.

In the study of Cheli et al. B16-F10 cells were stained with carboxyfluorescein succinimidyl ester (CFSE) and slow-cycling CFSE^high fraction was found to be enriched with Mitf^low cells, with high tumorigenic potential *in vivo* [29]. Interestingly, when we checked *Mitf* expression in PKH26⁻ and PKH26⁺ cells we found no difference between the two subsets (Fig. 1F). Consequently, there were no differences in the mRNA levels of *Tyr*, the major enzyme in the melanin synthesis pathway directly controlled by *Mitf* (Fig. 1F). This can be explained by the fact that we tested the SCC 10 days after PKH26 staining, while CFSE^high cells from Cheli et al. study were cultured only for 3 days [29]. Although PKH26⁺ and PKH26⁻ cells had a similar differentiation status, their progeny significantly differed in the expression of melanogenesis genes and PKH26⁺ progeny had decreased *Trp2* and *Gp100* (Fig. 3D). Expression of differentiation markers is a favorable factor in advanced-

stage melanoma outcome, thus decreased expression of these markers can indicate de-differentiation of cells and may contribute to increased melanoma aggressiveness [26].

Our data showed that PKH26$^+$ fraction was enriched with CD133$^+$ and ALDH^{high} cells (Fig. 1C). However, not all PKH26$^+$ cells expressed MIC markers (up to 27% of CD133$^+$PKH26$^+$ and 1.4% ALDH^{high}PKH26$^+$), suggesting that the expression of the MIC markers alone does not explain the behavior of SCC. Furthermore, we observed that the enrichment in the MIC fraction is lost in daughter cell lines formed from single PKH26$^+$ cells (Fig. 3B). This partial overlap in the expression of CSC markers in slow-cycling cells has been previously described in pancreas adenocarcinoma [30]. In human melanoma cell lines the SCC did not differ in expression of MIC markers (CD271 and CD133) [5]. Another study showed that melanoma SCC entirely express MIC marker CD271 but simultaneously non-SCC are composed of both CD271$^+$ and CD271$^-$ fractions [31]. Recently, CD133$^+$TRP-2$^+$ cells have been identified as a dormant melanoma phenotype in transgenic mice [32]. We observed high variability in the percentage of MIC subpopulations between experiments, which can be explained by high plasticity of melanoma cells [33,34]. Additionally, we showed that the progeny of PKH26$^+$ cells are not enriched in the PKH26$^+$ subpopulation, and the heterogeneity of PKH26$^+$ and PKH26$^-$ cells is restored after culture from single cells (Fig. 3A), consistent with previous studies [6,29]. Overall, our findings give further evidence that slow-cycling phenotype in melanoma is independent of the expression of MIC markers and proved the extraordinary plasticity of SCC melanoma cells.

Study of Perego et al. showed that when human melanoma cells were labeled with PKH26 and a million cells injected into SCID nude mice, the fluorescent signal measured with IVIS gradually disappeared in the primary tumor but was still present in distant organs in the form of metastases [5]. This invasive phenotype of SCC was also observed in a study where treatment-induced senescent melanoma cells were shown to be able to invade and metastasize in a WNT5A-dependent manner [35]. We observed a similar effect *in vitro*, where PKH26$^+$ cells disseminated from the primary clone after single-cell sorting, which resulted in the formation of more than one clone per well (Fig. 2D). We tried to understand this by using time-lapse 24 hours monitoring of clones, but we did not observe any differences in migration parameters between SCC and control cells (Supplementary Fig. 1). *In vivo* subcutaneous tumors derived from PKH26$^+$ cells formed metastases in up to 55% mice, meaning that progeny of PKH26$^+$ cells are able to disseminate from primary tumor. Overall, our results suggest that one of the hallmarks of murine melanoma SCC could be altered migratory potential. However this needs further validations.

Chemoresistance of SCC has been demonstrated *in vitro* and *in vivo* in human melanoma, glioblastoma, colorectal carcer and pancreas adenocarcinoma [7,25,30]. Treatment of melanoma cells with various drugs leads to increase in SCC expressing JARID1B demethylase, and inhibition of the respiratory chain in slow-cycling cells sensitizes melanoma to anticancer agents [36]. Our data demonstrates that progeny of SCC tends to increase chemoresistance toward doxorubicin (Fig. 4C) adding further insight into the importance of slow-cycling cells in melanoma chemoresistance.

In *in vivo* serial transplantations, only SCC initiated tumors from as little as 10 transplanted cells in primary recipients (Fig. 4). Consistently, others have shown that CFSE^{high} B16-F10 cells are tumorigenic, while CFSE^{low} cells failed to form tumors, even when 20 000 cells were transplanted [29]. Moreover, B16-F10 cell line can yield a high tumor incidence when single unfractionated cells are grown as clones and injected into syngeneic C57BL/6 mice [37]. Recently, our group reported that unselected B16-F10 cells are capable of forming tumors in a serial transplantation assay, and MIC markers fail to select cells with increased tumorigenicity [13]. Our results indicate that tumor formation by unfractionated murine melanoma cells can be explained in part by the presence of SCC, which increase tumorigenicity and incidents of delayed tumor growth (Fig. 4 B-D). Moreover, the ability to form tumors

by SCC was inherited by their progeny, which formed tumors in secondary and tertiary recipients, demonstrating the self-renewal potential of SCC. Interestingly, in human melanoma, slow-cycling JARID1B$^+$ cells and control JARID1B$^-$ cells had comparable tumorigenicity [6]. Those discrepancies between our study and human melanoma might be explained by different *in vivo* transplantation assays (xenotransplantation vs. syngeneic) that affect the outcome of melanoma tumor initiating properties [10]. Additionally, the differences might come from the fact that murine melanoma SCC are not marked by the higher expression of *Jarid1b* (Fig. 1F).

A limitation of our study is that despite the use of a targeted qPCR array detecting CSC-related genes, we were unable to find a marker that distinguishes murine SCC from non-SCC cells. This indicates once again that SCC phenotype is independent from the CSC phenotype and that other signaling pathways are responsible for the observed phenotype in murine melanoma. Moreover, temporary nature of SCC phenotype makes it hard to follow its regulators due to the dynamic switching on and off of this phenotype upon unspecified stimuli.

Taken together, our results show the existence of SCC in B16-F10 murine melanoma characterized by increased tumorigenic potential and self–renewal capabilities. In parallel with the reduced ability to form clones, SCC progeny tend to be more resistant to chemotherapeutics and have reduced expression of melanogenesis genes *in vitro*. This points to the importance of SCC in melanoma progression, confirming what was observed in human melanoma.

Author Contributions

Funding

Declaration of Competing Interest

The authors declare that they have no known competing financial interests or personal relationships that could have appeared to influence the work reported in this paper.

Acknowledgments

Supplementary materials

Supplementary material associated with this article can be found, in the online version, at doi:10.1016/j.neo.2022.100865.

References

[1] M. Arnold, et al., Global Burden of Cutaneous Melanoma in 2020 and Projections to 2040, JAMA Dermatology 158 (2022) 495–503.

[2] F. Ahmed, N.K Haass, Microenvironment-Driven Dynamic Heterogeneity and Phenotypic Plasticity as a Mechanism of Melanoma Therapy Resistance, Front. Oncol. 8 (2018) 1–7.

[3] A. Ahn, A. Chatterjee, M.R. Eccles, The Slow Cycling Phenotype: A Growing Problem for Treatment Resistance in Melanoma, Mol. Cancer Ther. 16 (2017) 1002–1009.

[4] S. Basu, Y. Dong, R. Kumar, C. Jeter, D.G. Tang, Slow-cycling (dormant) cancer cells in therapy resistance, cancer relapse and metastasis, Semin. Cancer Biol. 78 (2022) 90–103.

[5] M. Perego, et al., A slow-cycling subpopulation of melanoma cells with highly invasive properties, Oncogene 37 (2018) 302–312.

[6] A. Roesch, et al., A Temporarily Distinct Subpopulation of Slow-Cycling Melanoma Cells Is Required for Continuous Tumor Growth, Cell 141 (2010) 583–594.

[7] I. Puig, et al., TET2 controls chemoresistant slow-cycling cancer cell survival and tumor recurrence, J. Cinical Investig. 128 (2018) 3887–3905.

[8] M.R. Webster, et al., Paradoxical Role for Wild-Type p53 in Driving Therapy Resistance in Melanoma, Mol. Cell 77 (2020) 633–644 e5.

[9] M.E. Fane, et al., Stromal changes in the aged lung induce an emergence from melanoma dormancy, Nature 606 (2022) 396–405.

[10] E. Quintana, et al., Efficient tumour formation by single human melanoma cells, Nature 456 (2008) 593–598.

[11] E. Quintana, et al., Phenotypic heterogeneity among tumorigenic melanoma cells from patients that is reversible and not hierarchically organized, Cancer Cell 18 (2010) 510–523.

[12] M. Shackleton, E Quintana, Progress in understanding melanoma propagation, Mol. Oncol. 4 (2010) 451–457.

[13] A. Kusienicka, et al., Heme Oxygenase-1 Has a Greater Effect on Melanoma Stem Cell Properties Than the Expression of Melanoma-Initiating Cell Markers, Int. J. Mol. Sci. 23 (2022) 1–23.

[14] B. Stecca, R. Santini, S. Pandolfi, J Penachioni, Culture and isolation of melanoma-initiating cells, Curr. Protoc. Stem Cell Biol. 24 (2013) 3.6.1-3.6.12.

[15] U. Florczyk-Soluch, et al., Various roles of heme oxygenase-1 in response of bone marrow macrophages to RANKL and in the early stage of osteoclastogenesis, Sci. Rep. 8 (2018) 10797.

[16] K. Szade, et al., Spheroid-plug model as a tool to study tumor development, angiogenesis, and heterogeneity in vivo, Tumor Biol 37 (2016) 2481–2496.

[17] A. Zeuner, et al., Elimination of quiescent/slow-proliferating cancer stem cells by Bcl-XL inhibition in non-small cell lung cancer, Cell Death Differ 21 (2014) 1877–1888.

[18] C. Richichi, P. Brescia, V. Alberizzi, L. Fornasari, G. Pelicci, Marker-independent Method for Isolating Slow-Dividing Cancer Stem Cells in Human Glioblastoma, Neoplasia 15 (2013) 840–847.

[19] Pece, S. et al. Biological and Molecular Heterogeneity of Breast Cancers Correlates with Their Cancer Stem Cell Content. *Cell* 140, 62–73 (2010).

[20] N. Moore, S.Quiescent Lyle, slow-cycling stem cell populations in cancer: A review of the evidence and discussion of significance, J. Oncol. 2011 (2011).

[21] Y. Wei, et al., The Interaction between DNMT1 and High-Mannose CD133 Maintains the Slow-Cycling State and Tumorigenic Potential of Glioma Stem Cell, Adv. Sci. 9 (2022) 2202216.

[22] H.J. Xie, et al., HDAC1 inactivation induces mitotic defect and caspase-independent autophagic cell death in liver cancer, PLoS One 7 (2012) e34265.

[23] R. Sachdeva, et al., BMP signaling mediates glioma stem cell quiescence and confers treatment resistance in glioblastoma, Sci. Rep. 9 (2019) 14569.

[24] Y. Hu, G.K. Smyth, ELDA: Extreme limiting dilution analysis for comparing depleted and enriched populations in stem cell and other assays, J. Immunol. Methods 347 (2009) 70–78.

[25] N. Moore, J. Houghton, S. Lyle, Slow-Cycling Therapy-Resistant Cancer Cells, Stem Cells Dev 21 (2012) 1822–1830.

[26] H. Takeuchi, C. Kuo, D.L. Morton, H.J. Wang, D.S.B Hoon, Expression of Differentiation Melanoma-associated Antigen Genes Is Associated with Favorable Disease Outcome in Advanced-Stage Melanomas, Cancer Res 63 (2003) 441–448.

[27] V. Kuch, C. Schreiber, W. Thiele, V. Umansky, J.P. Sleeman, Tumor-initiating properties of breast cancer and melanoma cells in vivo are not invariably reflected by spheroid formation in vitro, but can be increased by long-term culturing as adherent monolayers, Int. J. Cancer 132 (2013) 94–105.

[28] N.K. Haass, et al., Real-time cell cycle imaging during melanoma growth, invasion, and drug response, Pigment Cell Melanoma Res 27 (2014) 764–776.

[29] Y. Cheli, et al., Mitf is the key molecular switch between mouse or human melanoma initiating cells and their differentiated progeny, Oncogene 30 (2011) 2307–2318.

[30] J.L. Dembinski, S. Krauss, Characterization and functional analysis of a slow cycling stem cell-like subpopulation in pancreas adenocarcinoma, Clin. Exp. Metastasis 26 (2009) 611–623.

[31] Y. Cheli, et al., CD271 is an imperfect marker for melanoma initiating cells, Oncotarget 5 (2014) 5272–5283.

[32] F. Flores-Guzmán, J. Utikal, V. Umansky, Dormant tumor cells interact with memory CD8+ T cells in RET transgenic mouse melanoma model, Cancer Lett 474 (2020) 74–81.

[33] M.A. Held, et al., Characterization of melanoma cells capable of propagating tumors from a single cell, Cancer Res 70 (2010) 388–397.

[34] L. Prasmickaite, et al., Human malignant melanoma harbours a large fraction of highly clonogenic cells that do not express markers associated with cancer stem cells, Pigment Cell Melanoma Res 23 (2010) 449–451.

[35] M.R. Webster, et al., Wnt5A promotes an adaptive, senescent-like stress response, while continuing to drive invasion in melanoma cells, Pigment Cell Melanoma Res 28 (2015) 184–195.

[36] A. Roesch, et al., Overcoming intrinsic multidrug resistance in melanoma by blocking the mitochondrial respiratory chain of slow-cycling JARID1Bhigh cells, Cancer Cell 23 (2013) 811–825.

[37] Y. Zhong, et al., Cancer stem cells sustaining the growth of mouse melanoma are not rare, Cancer Lett 292 (2010) 17–23.